Iron Nanoparticles Derived from Iron-Complexed Polymethylglutarimide To Produce High-Quality Lithographically Defined Single-Walled Carbon Nanotubes

Jennifer Q. Lu,*,† Nick Moll,† Qiang Fu,‡ and Jie Liu‡

Agilent Technologies, 3500 Deer Creek Road, Palo Alto, California 94304, and Chemistry Department, Duke University, Durham, North Carolina 27708

Received September 30, 2004
Revised Manuscript Received March 23, 2005

Carbon nanotubes (CNTs) with their exceptional electrical properties, chemical stability, and mechanical strength have attracted a great deal of attention. CNTs have been exploited as novel building blocks for various applications including composite materials,[1] battery electrode materials,[2] field emitters,[3] AFM tips,[4,5] nanoelectronics,[6,7] and nanoscale sensors.[8,9] Chemical vapor deposition (CVD) has gained popularity for CNT growth in which CNTs are grown selectively on catalytic sites. In a typical chemical vapor deposition process, carbon stocks, such as hydrocarbon gas, decompose at 500−1200 °C on catalytic sites to form CNTs. Therefore, the diameters, locations, and density of CNTs can theoretically be controlled by the sizes, locations, and density of catalysts.[10] Some progress has been made toward developing methods for controlling the diameters of CNTs. For example, discrete iron catalysts have been prepared from ferritin templates;[11] iron nanoparticles have been spontaneously formed by soaking a thermal silicon oxide surface in an iron salt solution[12] and recently iron catalysts with relatively controlled size have been prepared from a liquid micelle based approach.[13] All of these techniques provide some degree of controlling catalyst size and the corresponding CNT diameter, but do not provide a means to uniformly distribute catalysts and subsequent CNTs. Furthermore, with the use of most of the existing methods, it is difficult to disperse catalyst nanoclusters uniformly using a conventional spin-coating process and do not offer a manufactuable method to fabricate catalyst and CNT patterns on the micrometer or sub-micrometer scale at the wafer level, especially in systems when catalyst supports are used.[10,14]

In this report, we describe a method of generating iron nanoparticles derived from an iron-complexed polymer system. The size and density of iron nanoparticles are highly dependent on the complexation tendency of an iron source to a polymer, polymethylglutarimide (hereafter called PMGI) used in this study. We have found that an iron source such as iron nitrate is an effective material in generating high-density iron nanoparticles for CNT growth. The polymer not only serves as a template to control the size of the iron nanoparticles but also serves as a carrier to uniformly distribute iron-complexed polymer chains by spin-coating. On substrates prepared using this technique, we have been able to generate high-density and uniformly distributed CNT mats. More importantly, with use of a conventional semiconductor lithography process, iron-complexed PMGI patterns have been readily fabricated. CNT patterns have been successfully generated over a very large surface area using these lithographically defined catalyst regions.

Polymer carrier, PMGI, was purchased from Shipley under the trade name LOL1000 and diluted 1:1 by volume in cyclohexanone before use. Iron(III) chloride anhydrous and ferrocene were obtained from Sigma-Aldrich and iron(III) acetylacetone [denoted, $Fe(acac)_3$] and iron(III) nitrate·$9H_2O$ from Alfa Aesar. Iron compounds were carefully selected in this study for their different tendencies toward complexation. After an iron compound was dissolved into methanol, the solution was then added into 1:1 diluted LOL1000 to obtain an iron concentration of 0.0006 M. The solution was spin-coated at 4000 rpm on a 5000 Å thermal silicon oxide surface to obtain a 10 nm film. The thin film was then annealed for 15 h at 165 °C. The annealing condition was chosen to completely remove the solvent, to prevent intermixing with photoresist, and to improve the adhesion to the substrate. UV-ozonation was then used to remove the organic components and coalesce iron atoms into iron oxide nanoparticles.

The CNT growth was carried out in a CVD system as described previously.[15] A substrate with catalyst nanoparticles was first heated to 900 °C under 500 sccm H_2. A mixture of 800 sccm CH_4 and 20 sccm C_2H_4 was then added to the gas flow and maintained 10 min during the growth. After the

* To whom correspondence should be addressed. Tel: 650-485-3714. Fax: 650-485-8626. E-mail: Jennifer_lu@agilent.com.
† Agilent Technologies.
‡ Duke University.

(1) Huxtable, S. T.; Cahill, D. G.; Shenogin, S.; Xue, L. P.; Ozisik, R.; Barone, P.; Usrey, M.; Strano, M. S.; Siddons, G.; Shim, M.; Keblinski, P. *Nature Mater.* **2003**, *2*, 731.
(2) Honda, K.; Yoshimura, M.; Kawakita, K.; Fujishima, A.; Sakamoto, Y.; Yasui, K.; Nishio, N.; Masuda, H. *J. Electrochem. Soc.* **2004**, *151*, A532.
(3) Fan, S. S.; Chapline, M. G.; Franklin, N. R.; Tombler, T. W.; Cassell, A. M.; Dai, H. J. *Science* **1999**, *283*, 512.
(4) Hafner, J. H.; Cheung, C. L.; Woolley, A. T.; Lieber, C. M. *Prog. Biophys. Mol. Biol.* **2001**, *77*, 73.
(5) Dai, H. J.; Hafner, J. H.; Rinzler, A. G.; Colbert, D. T.; Smalley, R. E. *Nature* **1996**, *384*, 147.
(6) Appenzeller, J.; Knoch, J.; Martel, R.; Derycke, V.; Wind, S. J.; Avouris, P. *IEEE Trans. Nanotechnol.* **2002**, *1*, 184.
(7) Tans, S. J.; Dekker: C. *Nature* **2000**, *404*, 834.
(8) Chen, R. J.; Choi, H. C.; Bangsaruntip, S.; Yenilmez, E.; Tang, X. W.; Wang, Q.; Chang, Y. L.; Dai, H. J. *J. Am. Chem. Soc.* **2004**, *126*, 1563.
(9) Chen, R. J.; Bangsaruntip, S.; Drouvalakis, K. A.; Kam, N. W. S.; Shim, M.; Li, Y. M.; Kim, W.; Utz, P. J.; Dai, H. J. *Proc. Natl. Acad. Sci. U.S.A.* **2003**, *100*, 4984.
(10) Kong, J.; Soh, H. T.; Cassell, A. M.; Quate, C. F.; Dai, H. J. *Nature* **1998**, *395*, 878.
(11) Li, Y. M.; Kim, W.; Zhang, Y. G.; Rolandi, M.; Wang, D. W.; Dai, H. J. *J. Phys. Chem. B* **2001**, *105*, 11424.
(12) Choi, H. C.; Shim, M.; Bangsaruntip, S.; Dai, H. J. *J. Am. Chem. Soc.* **2002**, *124*, 9058.
(13) Choi, H. C.; Kim, W.; Wang, D. W.; Dai, H. J. *J. Phys. Chem. B* **2002**, *106*, 12361.
(14) Ago, H.; Nakamura, K.; Imamura, S.; Tsuji, M. *Chem. Phys. Lett.* **2004**, *391*, 308.
(15) Fu, Q.; Huang, S. M.; Liu, J. *J. Phys. Chem. B* **2004**, *108*, 6124.

10.1021/cm048280v CCC: $30.25
Published on Web 04/09/2005

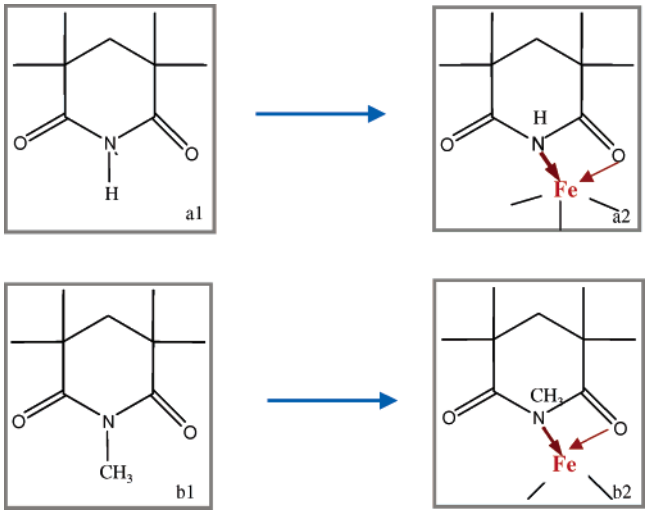

Figure 1. a1 and b1 are two main components of PMGI and a2 and b2 are the proposed structures after complexation.

growth, the mixture of hydrocarbon gases was switched off and the furnace was cooled to room temperature under the protection of H_2.

A DI-500 Digital Instrument atomic force microscope (AFM) was used to measure nanoparticle size and distribution. A Quantum 2000 X-ray photoemission spectrometer with an aluminum source was used for chemical composition analysis of nanoparticles. A Hitachi scanning electron microscope was employed to examine CNT density and patterned growth of CNTs. Micro-Raman analysis was used to investigate the overall quality and to obtain the diameters of CNTs. The analysis was conducted over a $\sim 1\ \mu m^2$ area using a laser with the excitation wavelength of 632 nm. The laser power was 2.0 mW and the integration time was 20 min.

PMGI is widely used as an underlayer for a bilayer liftoff process. The chemical structures for two of the main polymer repeat units are shown in Figure 1.[16] As can be seen, PMGI has multiple ligand sites on the polymer chain. Transition metals such as iron have energetically accessible d orbitals. These partially filled outer electronic orbitals provide a number of reaction pathways. To satisfy the 18 electron or inert gas rule, electron-rich ligands complex with the empty orbital of iron. The proposed coordination reaction product with iron species is shown in Figure 1.

We found that the tendency for complexation of iron species with PMGI plays a very important role in the resulting particle size, distribution, and overall yield. Figure 2 is a set of AFM images of nanoparticles formed on thermal oxide surfaces using PMGI with various iron sources. The mean and range of nanoparticle size produced from each system is tabulated in the inserted table. The size distribution of the particles produced from iron acetylacetonate is broad and the density of the particles is relatively low compared with those derived from either iron nitrate or iron chloride. The density of iron oxide clusters from ferrocene is the lowest. It is also apparent that particles obtained from

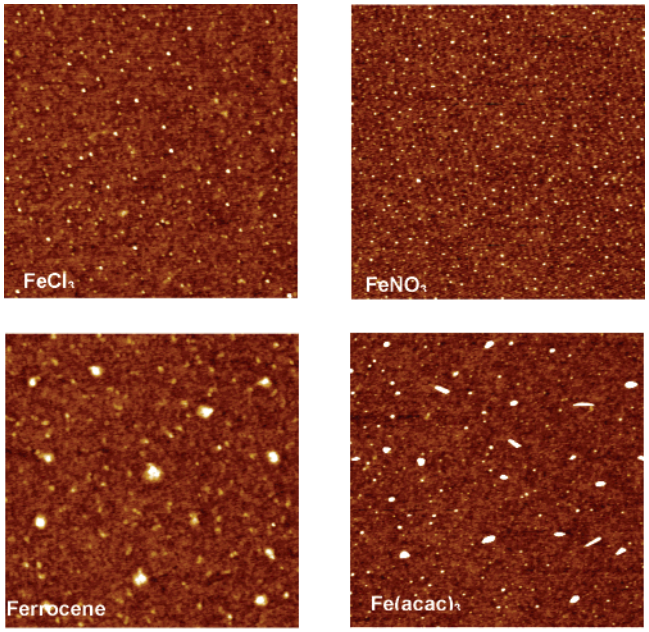

Iron precursor	Mean(nm)	Range of particle size (90% of population)
$Fe(NO_3)_3$	1.8	1.5-2.5nm
$FeCl_3$	2.3	2.0-3.6nm
$Fe(acac)_3$	3.2	2.0-9.0nm (bimodal distribution)
Ferrocene		Not well defined

Figure 2. Iron oxide nanoparticles derived from various iron compounds (2 μm $\times$ 2 μm scan, 5 nm in full scale). Particles size based on AFM height measurement.

ferrocene are not well-defined. This observation may be due to the inability of the iron organometallic compound to complex onto the PMGI polymer chains since ferrocene is coordinatively saturated. Furthermore, during polymer removal, ferrocene, which is a relatively volatile species by nature (bp = 249 °C), can easily be removed along with volatile organic species during UV−ozonation. Iron acetylacetonate, like ferrocene, is also a heavily complexed material but less volatile than ferrocene (bp = 343 °C). Not only are the acetylacetonate groups unlikely to dissociate from iron but also the steric hindrance from the bulky acetylacetonate ligands further reduces the chance of iron being complexed with PMGI. Therefore, the iron species in the poorly complexed system is likely to aggregate during the thermal annealing process. Consequently, iron oxide particles with larger and more variable size were condensed on the surface. The highest density of iron oxide nanoparticles with the smallest mean diameter was obtained from iron nitrate. This implies that iron nitrate complexed well with PMGI. It is consistent with the fact that iron nitrate is the most reactive species in our studies.[17] Unlike the organometallic materials, the iron species in iron nitrate and iron chloride can be complexed well with PMGI. In a comparison of iron nitrate and iron chloride, the nitrate groups in iron nitrate are more loosely attached to iron while the chlorine groups are more tightly complexed with iron. This is supported by the fact that 9 water molecules are attached to each iron nitrate molecule while only 6 water molecules are present in iron chloride in their hydrated forms.

(16) Brunsvold, W.; Lyons, C.; Conley, W.; Crikatt, D.; Skinner, M.; Uptmor, A. *Advances in resist technology and processing VI*; Reichmanis, E., Ed.; SPIE: Bellingham, WA, 1989; Vol. 1085, p 289.

(17) Schwertmann, U. Cornell, R. M. *Iron Oxides in the Laboratory*; Wiley-VCH: New York, 2000. Data from Aldrich and Alfa Aesar catalogues.

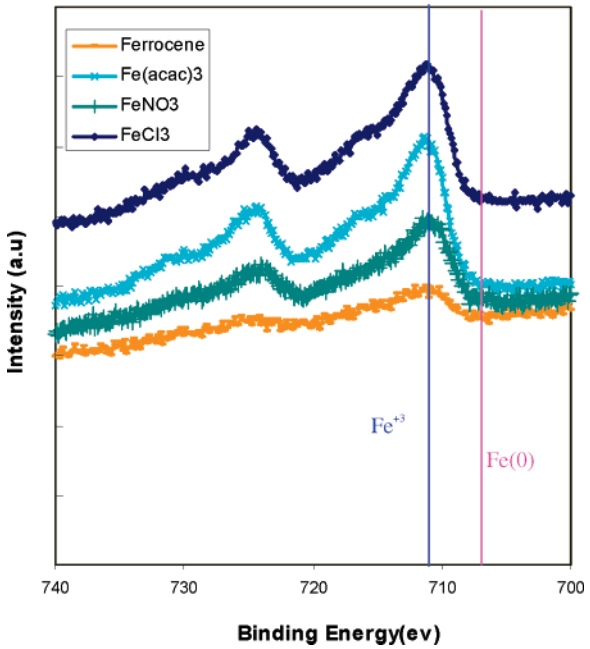

Figure 3. X-ray photoelectron spectra of iron oxide nanoparticles prepared from various iron compounds.

The result indicates that the uniformity of nanoparticle size increases with the tendency of complexation of iron species with PMGI and the nanoparticle density improves as well.

PMGI can be spin-coated to provide a high-quality, ultrathin, and uniform film. Complexation promotes the dispersion of iron species. More importantly, the polymer also serves as a template to control the number of iron species incorporated per chain and also ultimately determines the number of iron atoms in each nanoparticle. As can be seen, PMGI complexed with either iron nitrate or iron chloride has produced iron oxide nanoparticles with reasonably well-controlled size and distribution.

X-ray photoelectron spectra of resulting nanoparticles are shown in Figure 3. Fe $2p_{3/2}$ appears at 711 eV, indicating that iron is in the form of Fe_2O_3.[18,19] The low intensity of the Fe $2p_{3/2}$ peak from the surface prepared using ferrocene agrees well with the AFM result.

The iron oxide nanoparticles derived from this polymeric system has been proven to be excellent catalysts for CNT growth. Figure 4 is the SEM image of a CNT mat formed on a thermal silicon oxide surface using iron nitrate as an iron source. High-density and uniformly distributed CNTs with a density of 20 tubes per μm^2 has been produced and the uniform density is maintained across the entire surface.

Micro-Raman analysis was carried out to characterize the carbon nanotubes. SWNTs show characteristic low-energy peaks in their Raman spectra corresponding to the radial breathing vibrational modes with A_{1g} symmetry.[19,20] Radial breathing vibration is unique to nanotubes with one or few walls. Since the frequency of the radial breathing mode (RBM) is inversely proportional to CNT diameter, the diameters of CNTs can be estimated by measuring the RBM

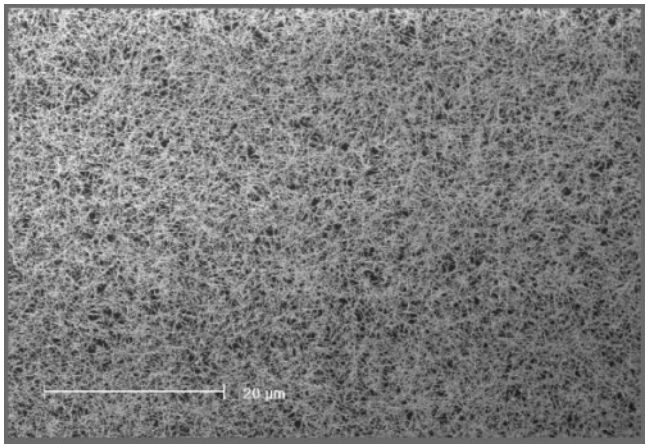

Figure 4. Carbon nanotubes grown from iron oxide nanoparticles derived from PMGI/$Fe(NO_3)_3$.

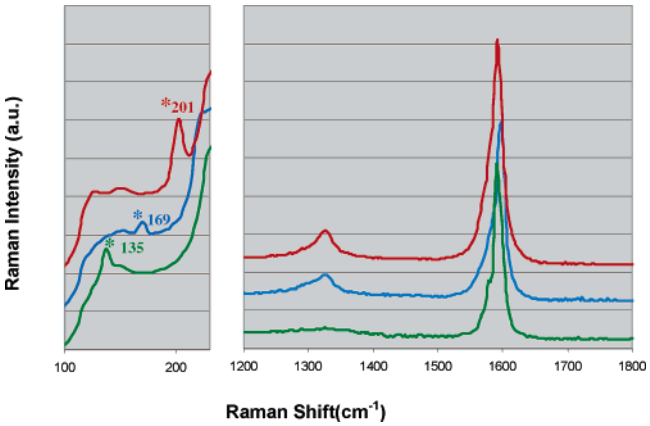

Figure 5. Micro-Raman spectra of carbon nanotubes grown from iron oxide nanoparticles derived from PMGI/$Fe(NO_3)_3$.

frequencies. The tube diameters are estimated using the relationship $d(\text{nm}) = 248\ \text{cm}^{-1}/\omega_{\text{RBS}}$ shift.[20,21] A slight shift to lower frequency in the RBM due to overlapping of tubes was ignored.[22] The tube diameters based on Raman spectroscopic analyses ranged from 1.2 to 1.8 nm. The peaks at 134, 169, and 201 cm^{-1} in Figure 5 were observed in spectra collected at different regions and were identified as SWNTs with diameters of 1.24, 1.45, and 1.85 nm, respectively. The CNT diameters are slightly smaller than the sizes of the nanoparticles, which is possibly due to the sublimation of iron before growth or particle shrinkage due to the conversion of iron oxide to iron. The strong intensity of the G band at 1590 cm^{-1} corresponds to an in-plane oscillation of carbon atoms in the graphene sheet. The low intensity of the D band at 1350 cm^{-1} indicates a low level of defects or dangling bonds.[20,21,23] The relatively high laser power used for these analyses might artificially enhance the D band due to laser damage. Nevertheless, the ratio of G/D is very high, indicating that this type of catalyst derived from iron-complexed PMGI produces high-quality single-walled CNTs.

(18) Konno, H.; Nagayama, M. J. *Electron Spectrosc. Relat. Phenom.* **1980**, *18*, 341.
(19) Paparazzo E. J. *Phys. D* **1987**, *20*, 1091.
(20) Dresselhaus, M. S.; Eklund, P. C. A*dv. Phys.* **2000**, *49*, 705.
(21) Dresselhaus G.; Dresselhaus, M. S. In *Science and Applications of Nanotubes*; Tománek, D., Enbody, R. J., Eds.; Kluwer Academic: New York, 2000, p 275.
(22) Rao, A. M.; Chen, J.; Richter, E.; Schlecht, U.; Eklund, P. C.; Haddon, R. C.; Venkateswaran, U. D.; Kwon, Y. K.; Tomanek, D. *Phys. Rev. Lett.* **2001**, *86*, 3895.
(23) Souza, A. G.; Jorio, A.; Samsonidze, G. G.; Dresselhaus, G.; Saito, R.; Dresselhaus, M. S. *Nanotechnology* **2003**, *14*, 11.

Since PMGI is not miscible with photoresist, it is widely used for liftoff processes.[16] Because of this immiscibility, photoresists can be directly coated and patterned on top of a PMGI layer. Pattern transfer into an iron-complexed PMGI layer can be done by using a longer development time during the resist development step. Since PMGI has much higher solubility in the developer than unexposed resist, slight overdevelopment can completely remove PMGI in the exposed area without attacking resist patterns. Figure 6a shows the iron-containing PMGI patterns produced using this over-development process after removing the resist with acetone. Figure 6b is the corresponding SEM image of CNT patterns and Figure 6c is another example of CNTs grown from lithographically defined catalyst lines. We have successfully demonstrated that catalyst locations can be defined in one simple lithographic step. Furthermore, with use of the excellent processability of a polymeric material, catalyst and resulting CNT density can be potentially controlled at the wafer level. This polymer-based approach is a simple and yet robust process with excellent potential to fabricate CNTs at lithographically defined locations in a reproducible and highly manufacturable manner.

In summary, we have developed a novel system to produce iron oxide nanoparticles using a polymer-based approach. In our studies, a polymer, PMGI, serves as a template to control the number of iron atoms that can be incorporated onto the polymer chain, and also acts as a carrier to uniformly disperse the iron-complexed polymer chains on a surface by simple spin-coating. After the removal of all the organic components, uniformly distributed iron nanoparticles with reasonably controlled size have been produced. We have found that the complexation reaction is essential to obtain small and yet high-density nanoparticles. Our studies have shown that the system in which iron nitrate is complexed with PMGI produces the most uniform iron oxide nanoclusters. The excellent processability of the polymeric material offers the potential to control catalyst density and CNT density at the wafer level. We have developed a process in which catalyst locations can be defined by a single photolithography step. As a result, the spatially selective growth of CNTs has been demonstrated. Since the overall process is fully compatible with conventional device fabrication, this method can be easily integrated into manufacturing to fabricate highly uniform carbon nanotube patterns on any wafer format.

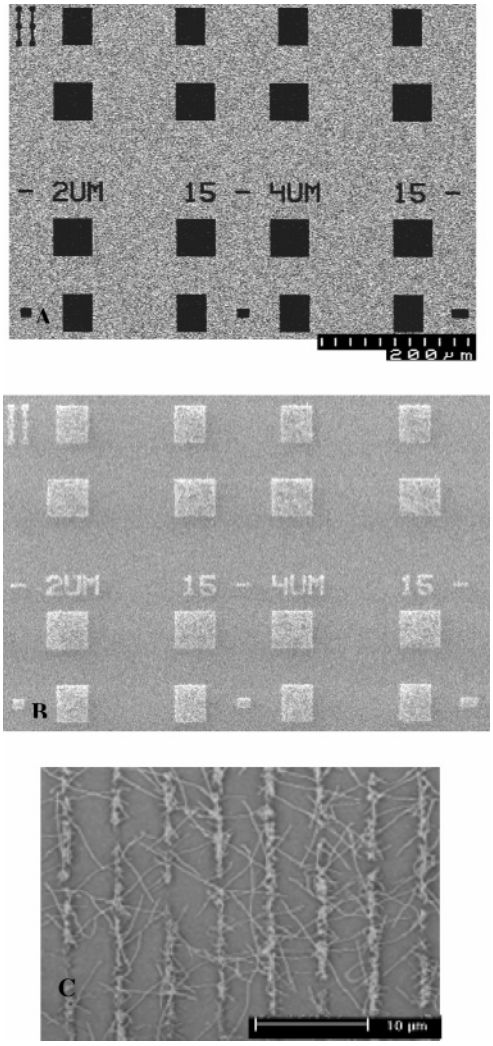

Figure 6. (A) Fe-containing catalyst pattern (600 × 420 μm), (B) corresponding patterned CNT mats (600 × 420 μm), and (C) lithographically selective growth of CNTs from catalyst lines.

Acknowledgment. We would like to thank Thomas Kopley for generating the Matlab program for AFM image analysis and Grant Girolami for SEM work. Jennifer Lu and Nick Moll would like to thank Rolf Jaeger for management support.

CM048280V